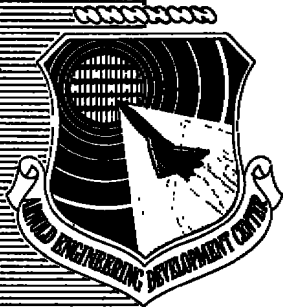


JUL 15 1994

Cy1



STUDY OF SIX-COMPONENT INTERNAL STRAIN GAGE BALANCES FOR USE IN THE HIRT FACILITY

**GENERAL DYNAMICS CORPORATION
CONVAIR AEROSPACE DIVISION
SAN DIEGO, CALIFORNIA 42138**

July 1975

Final Report for Period April 1973 – February 1974

Approved for public release; distribution unlimited.

**Property of U. S. Air Force
AEDC LIBRARY
F40600-75-C-0001**

Prepared for

**ARNOLD ENGINEERING DEVELOPMENT CENTER (DY)
AIR FORCE SYSTEMS COMMAND
ARNOLD AIR FORCE STATION, TENNESSEE 37389**

NOTICES

When U. S. Government drawings specifications, or other data are used for any purpose other than a definitely related Government procurement operation, the Government thereby incurs no responsibility nor any obligation whatsoever, and the fact that the Government may have formulated, furnished, or in any way supplied the said drawings, specifications, or other data, is not to be regarded by implication or otherwise, or in any manner licensing the holder or any other person or corporation, or conveying any rights or permission to manufacture, use, or sell any patented invention that may in any way be related thereto.

Qualified users may obtain copies of this report from the Defense Documentation Center.

References to named commercial products in this report are not to be considered in any sense as an endorsement of the product by the United States Air Force or the Government.

This final report was submitted by General Dynamics Corporation, Convair Aerospace Division, San Diego, California 92138, under contract F40600-72-C-0015 (Phase II), with the Arnold Engineering Development Center (AEDC) Arnold Air Force Station, Tennessee 37389. Mr. Ross G. Roepke, DYX, was the AEDC Project Scientist.

This report has been reviewed by the Information Office (OI) and is releasable to the National Technical Information Service (NTIS). At NTIS, it will be available to the general public, including foreign nations.

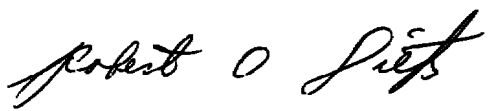
APPROVAL STATEMENT

This technical report has been reviewed and is approved for publication.

FOR THE COMMANDER



ROSS G. ROEPKE
Requirements Planning Division
Directorate of Technology



ROBERT O. DIETZ
Director of Technology

UNCLASSIFIED

| REPORT DOCUMENTATION PAGE | | READ INSTRUCTIONS BEFORE COMPLETING FORM |
|---|----------------------|--|
| 1 REPORT NUMBER AEDC-TR-75-63 | 2 GOVT ACCESSION NO. | 3. RECIPIENT'S CATALOG NUMBER |
| 4 TITLE (and Subtitle) STUDY OF SIX-COMPONENT INTERNAL STRAIN GAGE BALANCES FOR USE IN THE HIRT FACILITY | | 5 TYPE OF REPORT & PERIOD COVERED Final Report - April 1973 - February 1974 |
| | | 6 PERFORMING ORG. REPORT NUMBER CASD-AFS-73-009 |
| 7 AUTHOR(s) M. L. Kuszewski, P. J. Mole, and S. A. Griffin | | 8. CONTRACT OR GRANT NUMBER(s) F40600-72-C-0015 (Phase II) |
| 9 PERFORMING ORGANIZATION NAME AND ADDRESS General Dynamics Corporation Convair Aerospace Division San Diego, California 92138 | | 10 PROGRAM ELEMENT, PROJECT, TASK AREA & WORK UNIT NUMBERS Program Element 65802F |
| 11 CONTROLLING OFFICE NAME AND ADDRESS Arnold Engineering Development Center(DYFS) Air Force Systems Command Arnold Air Force Station, Tennessee 37389 | | 12 REPORT DATE July 1975 |
| | | 13. NUMBER OF PAGES 39 |
| 14 MONITORING AGENCY NAME & ADDRESS(if different from Controlling Office) | | 15. SECURITY CLASS. (of this report) UNCLASSIFIED |
| | | 15a DECLASSIFICATION/DOWNGRADING SCHEDULE N/A |
| 16 DISTRIBUTION STATEMENT (of this Report) Approved for public release; distribution unlimited. | | |
| 17 DISTRIBUTION STATEMENT (of the abstract entered in Block 20, if different from Report) <i>2. Strain gage balances.</i> | | |
| 18 SUPPLEMENTARY NOTES Available in DDC | | |
| 19 KEY WORDS (Continue on reverse side if necessary and identify by block number) <div style="display: flex; justify-content: space-between;"> <div> strain gages balance wind tunnels Reynolds number </div> <div> accuracy loads(force) structural properties costs </div> </div> | | |
| 20 ABSTRACT (Continue on reverse side if necessary and identify by block number) <p>The need for a High Reynolds Number Transonic Wind Tunnel (HIRT) has been recognized throughout the industry for some years. The proposed HIRT facility at Arnold Engineering Development Center will provide a much needed tool for the study of phenomena sensitive to Reynolds number. The usefulness of the HIRT facility will be largely influenced by the ability of industry to design and build wind-tunnel models and internal strain gage balances capable</p> | | |

UNCLASSIFIED

UNCLASSIFIED

20. ABSTRACT (Continued)

of operating within the severe environment of the tunnel. The balance concept selected for this study has been used for the past ten years at General Dynamics and is known as a two-shell balance. Information presented is based on experience together with the results of experimental work in progress at General Dynamics. Balance load capability is presented in relation to balance diameter together with a typical load rhombus. Combined load ratios are examined, and alternate curves are presented to show increased balance capacity in selected primary components, with decreased capacity in the secondary components. Balance sketches and stress reports are included. Balance capabilities are illustrated. High capacity balances are defined as 6-component balances with normal force divided by diameter squared equal to $1,700 \text{ lb/in.}^2$. The study concluded that high capacity balances suitable for use in the HIRT facility can be built at reasonable cost using present-day technology and materials without seriously degrading balance accuracy due to high capacity. However, further study of balances less than 3 inches in diameter is necessary. In this size range higher load capability is desirable, and alternate design concepts may prove more advantageous.

PREFACE

This report describes the work performed on Air Force contract F40600-72-C-0015 (Phase II) by the Convair Aerospace division of General Dynamics Corporation, San Diego operation, San Diego, California. The report is identified by contractor's number CASD-AFS-73-009.

This study is one of a four-part program conducted for Phase II. The other three studies are:

- a. AEDC-TR-75-60, "Study of Multipiece, Flow-Through Wind Tunnel Models for HIRT."
- b. AEDC-TR-75-61, "Study of Expected Data Precision in the Proposed AEDC HIRT Facility."
- c. AEDC-TR-75-62, "Study of HIRT Model Aeroelastic Characteristics in Reference to the Aeroelastic Nature of the Flight Vehicle."

The work was administered by the Department of the Air Force, Headquarters, Arnold Engineering Development Center (TMP), Arnold Air Force Station, Tennessee with Mr. Ross G. Roepke, AEDC (DYX), as the Air Force technical representative.

This program was conducted in the research and engineering department of Convair Aerospace Division and was managed by Mr. S. A. Griffin. The work for this study was accomplished between May and November 1973.

Principal contributors to this study include:

- Wind Tunnel Design: M. L. Kuszewski, P. J. Mole, S. A. Griffin (Authors)
- Aerodynamics: G. J. Fatta
- Computer Group: W. A. Yates
- Publications: A. Wilson

The reproducibles used in the reproduction of this report were supplied by the authors.

TABLE OF CONTENTS

| <u>Section</u> | | <u>Page</u> |
|----------------|---|-------------|
| I | INTRODUCTION | 5 |
| II | PROGRAM ORGANIZATION | 6 |
| III | DESIGN PARAMETERS | 7 |
| | 3.1 BALANCE TYPE | 7 |
| | 3.2 MATERIALS | 7 |
| | 3.3 LOADS AND SAFETY FACTORS | 7 |
| | 3.4 BRIDGE OUTPUTS | 7 |
| | 3.5 GAGE STRESSES | 8 |
| IV | BASIC DESIGN PHILOSOPHY | 9 |
| | 4.1 BALANCE CONCEPT | 9 |
| | 4.2 MATERIAL SELECTION | 9 |
| | 4.3 SAFETY FACTORS | 17 |
| V | BALANCE LOAD CAPACITIES | 18 |
| VI | STRESS ANALYSIS | 23 |
| | 6.1 BALANCE STRESSES | 23 |
| | 6.1.1 Web Stress Calculations | 23 |
| | 6.1.2 Ear Stresses | 24 |
| | 6.1.3 Inner Rod Stresses | 24 |
| | 6.1.4 Brazed Joint Stresses | 25 |
| | 6.1.5 Balance-to-Model Pins | 26 |
| | 6.2 BRIDGE OUTPUTS | 26 |
| | 6.3 BALANCE DEFLECTION | 26 |
| | 6.4 BALANCE GAGE STRESS | 26 |
| VII | BALANCE-TO-STING JOINT | 28 |
| | 7.1 CLUTCH FACE JOINT | 28 |
| | 7.2 TAPER JOINT | 31 |
| | 7.3 COMPARISON OF BALANCE-TO-STING JOINTS | 32 |
| VIII | COMPARISON OF BALANCE COST ESTIMATES | 33 |
| IX | ESTIMATE OF BALANCE ACCURACY | 34 |
| X | CONCLUSIONS | 36 |

LIST OF FIGURES

| <u>Figure</u> | | <u>Page</u> |
|---------------|--|-------------|
| 1 | Program Operations Chart | 6 |
| 2 | Balance Geometry | 11 |
| 3 | C-120-2.50-A Two-Shell Balance | 13 |
| 4 | Strain Gage Fatigue Life Curves | 16 |
| 5 | Apparent Strain and Gage Factor of Strain Gage Alloys versus Temperature | 17 |
| 6 | Typical Load Rhombus for Combined Loading Condition | 19 |
| 7 | Normal Force Capacity versus Balance Diameter | 20 |
| 8 | Typical Load Rhombus for Specified Loading Condition | 21 |
| 9 | Effect of Center Hole on Balance Capacity | 22 |
| 10 | Clutch Face Joint for 3.50-in. -dia. Balance | 28 |
| 11 | Taper Joint for 3.50-in. -dia. Balance | 31 |

LIST OF TABLES

| <u>Table</u> | | <u>Page</u> |
|--------------|---|-------------|
| 1 | Balance Material and Properties | 14 |
| 2 | Balance Load Ratios and Balance Loads for Combined Loading Condition (Normal Force as a Base) | 19 |
| 3 | Load Ratios and Balance Loads for Specified Loading Condition (Normal Force as a Base) | 22 |
| 4 | Safety Factor Summary | 24 |
| 5 | Summary of Web Stresses | 24 |
| 6 | Ear Stresses | 25 |
| 7 | Inner Rod Stresses | 25 |
| 8 | Brazed Joint Analysis | 25 |
| 9 | Balance-to-Model Pin Analysis | 26 |
| 10 | Bridge Outputs | 26 |
| 11 | Balance Deflections | 27 |
| 12 | Balance Gage Stress | 27 |
| 13 | Standard Deviations (1 σ) of Three Two-Shell Balances | 34 |

ABBREVIATIONS AND SYMBOLS

38

SECTION I

INTRODUCTION

A high Reynolds number Ludwig tube transonic wind tunnel (HIRT) is being proposed for construction at Arnold Engineering Development Center, Tullahoma, Tennessee.* Previous studies of the facility have indicated a need for strain gage balances whose high capacity does not result in degradation of accuracy or excessive costs. High loads, combined with high pitch rates, short run times, and the need for accurate drag data make balance requirements very demanding.

The objective of this study was to perform a preliminary design analysis on a family of high-capacity balances specifically to meet the demanding environmental conditions of the HIRT facility. The balance diameters selected for study are 1-1/2, 2-1/2, 3-1/2, and 4-1/2 inches. Section III reviews the balance design parameters; particularly materials, safety factors, bridge outputs, and gage stresses. Section IV illustrates the selected balance and outlines the reasons for selecting the two-shell concept.

Balance design study results are discussed in Section V and include:

- a. Load ratios in terms of normal force.
- b. Balance diameter versus load.
- c. Load rhombuses.

Basic structural analyses, deflections, gage stresses and component output calculations are presented in Section VI. The balance-to-sting joint concepts are analyzed and compared in Section VII.

In Section VIII, balance cost estimates are given on the basis of comparisons between high capacity balances for the HIRT facility, and existing transonic wind tunnel facilities.

Since accuracy of the balance is of prime importance, Section IX reviews probable accuracies to be expected from these balances. Also a general discussion is presented of accuracy degradation as data points of less than full capacity loads are recorded.

Conclusions are presented in Section X.

*Since completion of this report by Convair, a final decision was made not to construct the HIRT at AEDC in favor of a continuous cryogenic wind tunnel, site as yet undetermined.

SECTION II

PROGRAM ORGANIZATION

The design of a family of six-component internal strain gage balances for the HIRT facility was conducted by a program team established within the research and engineering department of Convair Aerospace division of General Dynamics.

The program operations chart, Figure 1, illustrates the flow of information from the various technical groups, through design, to the final report.

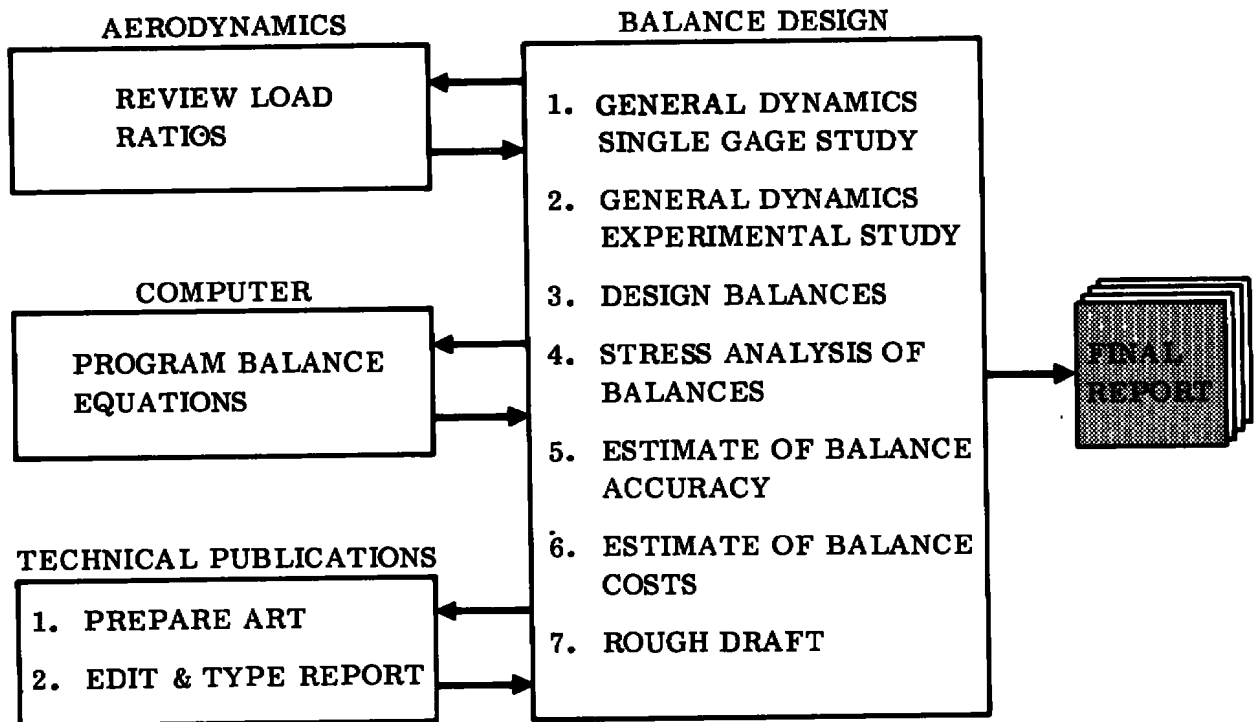


Figure 1. Program Operations Chart

SECTION III

DESIGN PARAMETERS

This design study of high-capacity internal strain gage balances for a HIRT facility is based on present-day technology and materials. The objective of this study was to select an existing balance design concept and to optimize it for use in the HIRT facility.

3.1 BALANCE TYPE

The internal strain gage balances discussed here are preliminary designs of the General Dynamics two-shell concept. This balance concept can be briefly described as two separate concentric cylindrical shells connected by strain gaged flexures. The outer shell is generally attached to the model and the inner shell is attached to the tunnel support. Therefore all model loads pass through the gaged flexures.

3.2 MATERIALS

A high tensile yield stress 18Ni-300 grade maraging steel is used as a baseline material for stress, deflection, and cost analysis of these balances (Reference 1). A Karma alloy strain gage, not previously used on balances at General Dynamics Convair Aerospace division, is used as the basic strain gage in all discussions of gage stress and gage fatigue life (see paragraph 3.5).

3.3 LOADS AND SAFETY FACTORS

All balance loads are such that a safety factor of 2.00 on yield is maintained on the balances under the simultaneous application of combined loads, as defined by the load ratios in Section V, Table 2.

3.4 BRIDGE OUTPUTS

Pitching moment, normal force, and axial force are of primary concern with respect to accuracy. The other three components (side force, yawing moment, and rolling moment) are less critical. Therefore, to allow more flexibility in the design of the balances, the following desired bridge outputs, with 6 volts input, are established:

| | | | |
|----------------------|----------|----------------|----------|
| Normal force forward | = 5 mv | Side force aft | = 3.5 mv |
| Normal force aft | = 5 mv | Roll moment | = 2.0 mv |
| Side force forward | = 3.5 mv | Axial force | = 5 mv |

-
1. 18% Nickel Ultra High Strength Maraging Steels, VASCOMAX 200-250-300-350, Vanadium-Pacific Steel Co., Montebello, California.

3.5 GAGE STRESSES

Constantan foil strain gages were reviewed and compared with Karma gages. Gage manufacturers were consulted, and it was concluded that the design and maximum allowable combined load gage stress on 18Ni-300 grade steel would be:

- a. 55,000 psi Constantan
- b. 82,000 psi Karma

The significant increase in gage stress allowed by use of the Karma gage gives the designer the freedom to design the balance to a higher working stress. Available higher strength materials can now be used to their full allowables, with safety factors of 2.00 on yield.

SECTION IV

BASIC DESIGN PHILOSOPHY

The selected internal strain gaged balance design is a logical candidate for the family of balances required for the HIRT facility. The balance geometry is presented in Figure 2; a photo of the C-120-2.50-A balance is shown in Figure 3. The following discussion develops the design parameters noted in Section III.

4.1 BALANCE CONCEPT

The two-shell balance concept has a number of significant advantages inherent in its design. For example:

- a. Its high stiffness alleviates the problem of model/sting clearance and also provides a relatively high natural frequency.
- b. The design is very versatile in that provisions can be made to incorporate a passage through the balance center.
- c. Failure of the balance flexures proves to be noncatastrophic to the model.
- d. The load ratios of a typical HIRT model best lend themselves to a two-shell balance (in particular, the high side force and yawing moment).

In each of these points the two-shell design has a definite advantage over the beam balance. The beam balance on the other hand, has the following advantages:

- a. Higher load capabilities at the smaller diameters.
- b. Balance cost is approximately 15 percent less.

General Dynamics Convair Aerospace division has two-shell data collected over the past ten years. The single gage process, which has been developed to determine minimum interaction bridges, also provides a backlog of stress information on which to base this study.

The two-shell balance has been an important instrument in the General Dynamics wind tunnel balance inventory. The single gaging process has been performed on more than 20 of these balances. Past studies of this data have led to the development of equations that accurately predict the stresses of this indeterminant structure.

4.2 MATERIAL SELECTION

The baseline metal chosen for the balance family is 18-Ni 300 grade double maraging steel. Material properties, shown in Table 1, include high tensile strength, corrosion resistance, stability of dimensions over the HIRT tunnel temperature range, availability

| ITEM | BALANCE | | | |
|----------------------|-------------------|-------------------|-------------------|-------------------|
| | 1.50 in. dia. | 2.50 in. dia. | 3.50 in. dia. | 4.50 in. dia. |
| A | 4.368 | 4.751 | 5.182 | 5.596 |
| B | 8.839 | 9.605 | 10.467 | 11.295 |
| BRAZL | 1.135 | 1.385 | 1.635 | 1.885 |
| C | 0.375 | 0.438 | 0.500 | 0.625 |
| DIA | 1.500 | 2.500 | 3.500 | 4.500 |
| DISTW/2 | 3.000 | 3.000 | 3.000 | 3.000 |
| EARLG | 0.233 | 0.366 | 0.547 | 0.711 |
| KEY SLOT | 0.250 | 0.313 | 0.438 | 0.500 |
| OVERALL LENGTH | 11.149 | 13.415 | 15.777 | 18.105 |
| PIN DIMENSIONS | 0.250 DIA x 0.125 | 0.313 DIA x 0.200 | 0.438 DIA x 0.350 | 0.500 DIA x 0.500 |
| SLOT | 0.020 | 0.020 | 0.020 | 0.020 |
| SPLIT CUT | 0.090 | 0.090 | 0.100 | 0.100 |
| TAPER | 0.625 IN/FT | 0.625 IN/FT | 0.625 IN/FT | 0.625 IN/FT |
| TAPER LENGTH | 2.250 | 3.750 | 5.250 | 6.750 |
| TAPER MAJOR DIAMETER | 1.200 | 1.900 | 2.450 | 3.050 |
| TAPER MINOR DIAMETER | 1.083 | 1.705 | 2.177 | 2.698 |
| TIRID | 0.390 | 0.390 | 0.390 | 0.390 |
| TIRN | 1.150 | 1.850 | 2.420 | 3.000 |
| TNOPW | 3 | 4 | 4 | 5 |
| TOSID | 1.180 | 1.880 | 2.450 | 3.030 |
| TOSOD | 1.470 | 2.470 | 3.470 | 4.470 |
| WL | 0.525 | 0.750 | 1.250 | 1.500 |
| WT | 0.096 | 0.236 | 0.392 | 0.590 |
| WW | 0.075 | 0.118 | 0.186 | 0.195 |
| Y | 1.277 | 2.117 | 2.844 | 3.620 |

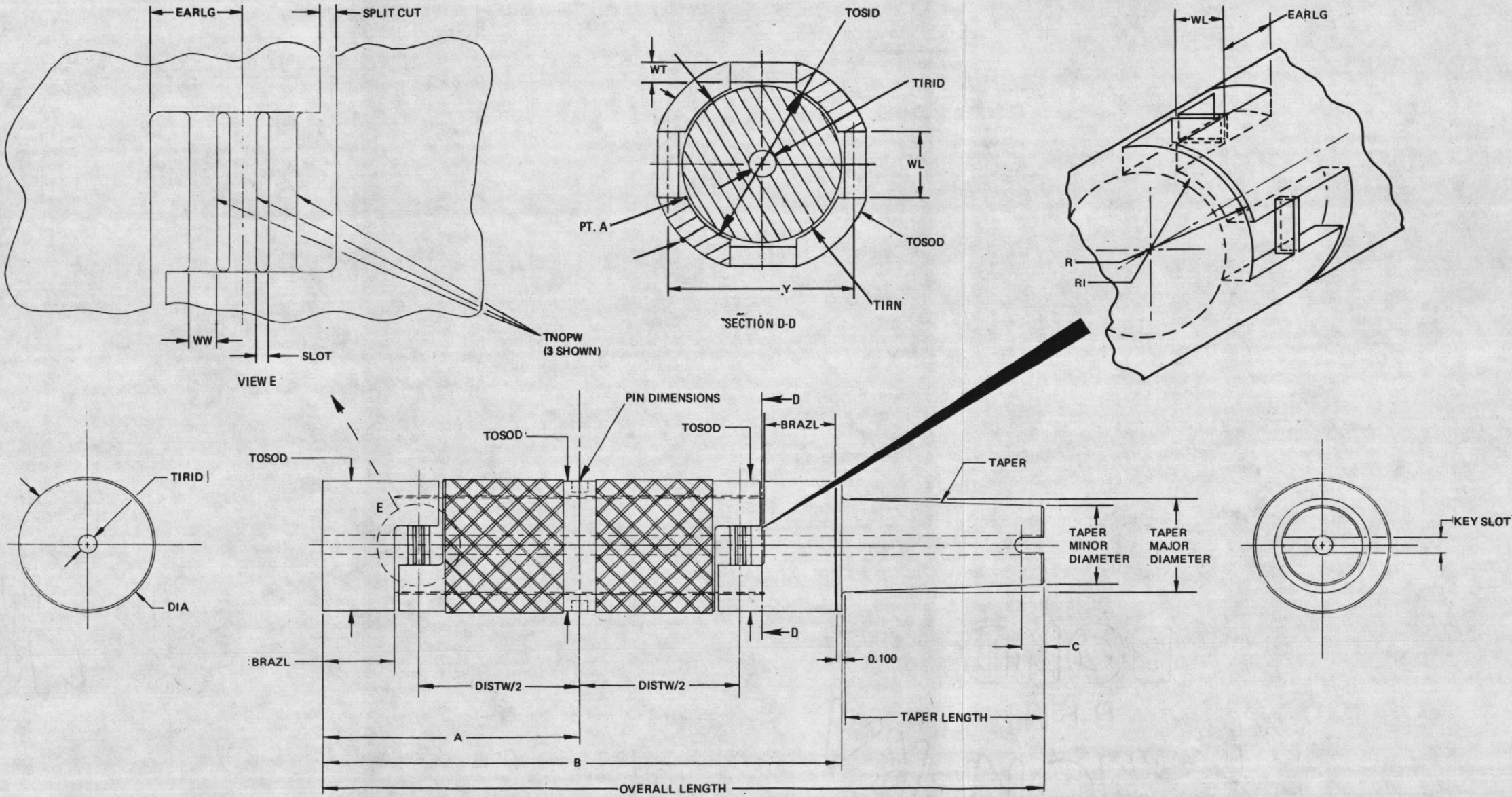


Figure 2. Balance Geometry

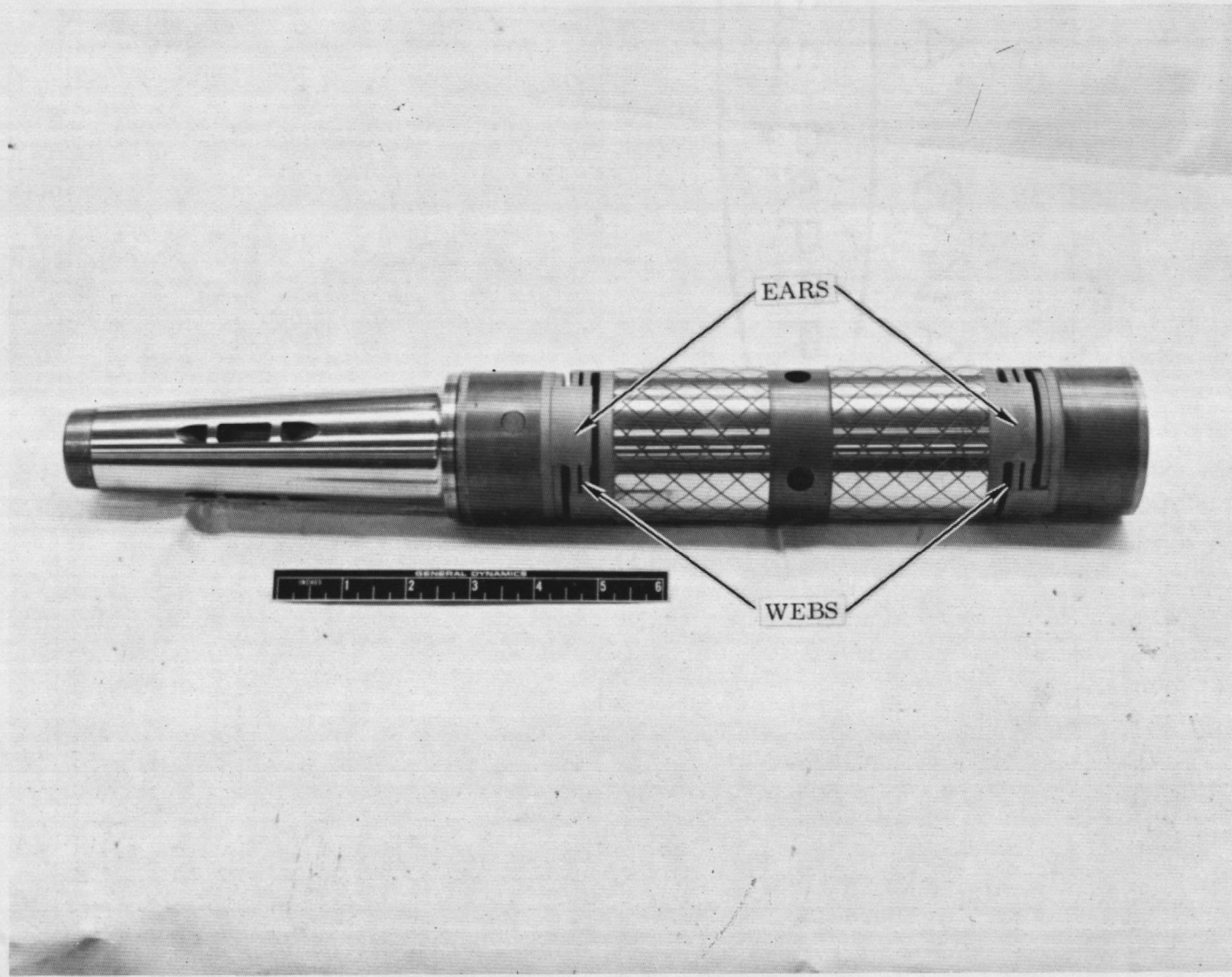


Figure 3. C-120-2.50-A Two-Shell Balance

in various sizes and shapes, and ease of fabrication. It is noted that other new materials may be developed that will have improved properties. Therefore, potential balance materials should be reviewed as they appear on the market.

Strain gages are as important to the balance as the material. Working stresses of the high-strength 18-Ni 300 grade steel are very high. This fact combined with the low safety factors allowed in a HIRT facility mean that the strain gages must operate for all combined loads at higher gage stresses to make full use of the material working stresses. Certain design techniques can be used to take advantage of some of the working stress without substantially increasing the gage stresses. However, the most advantageous way to use the material working stress is to use a higher gage stress. In order to use this higher gage stress, it is important to examine the properties of the strain gages at higher stress levels.

The Constantan gages at General Dynamics are used where the maximum gage stress for combined loads is designed for 55,000 psi. With the need for higher working gage stresses, it was necessary to examine the available strain gages to find a type possessing better properties at the higher stress level without sacrificing the other qualities. The Karma alloy strain gage is therefore recommended.

Table 1. Balance Material and Properties

| Material | 18-Ni 300 Grade (Reference 1) |
|---------------------------------------|-------------------------------|
| F_{tu} (ksi) | 300 |
| F_{ty} (ksi) | 280 |
| F_{su} (ksi) | 170 |
| Elongation (%) | 5 |
| E (10^6 psi) | 27.0 |
| G (10^6 psi) | 10.2 |
| Charpy V-notch (ft-lb) | 17 |
| K_{IC} (ksi $\sqrt{\text{in.}}$) | 60 |
| O & T Machinability | Good |
| Weldability | Good |
| Availability (bar, plate, or billets) | Good |

The Karma gage has high fatigue life together with the properties required for balances. Figure 4 illustrates the advantage of Karma gages over Constantan gages. The fatigue life curves provide a direct comparison with the Karma gage, showing an improved fatigue life at a higher strain level. This substantial gain becomes very important when fatigue life is used as the criteria for allowable gage stress. The allowable stress level for Karma gages is established here as that which provides the same fatigue life

expectancy without zero shifts, as with the Constantan gages used in standard practice today.

The Constantan gage design stress level is:

$$f_{t_c} = 55,000 \text{ psi}$$

The equivalent strain level is:

$$\epsilon_{t_c} = \frac{55,000}{27,000,000} = 2,000 \text{ microinch/inch}$$

The fatigue life at this strain level is approximately 10^3 cycles (Reference 2). The Karma gage strain level for equivalent fatigue life is:

$$\epsilon_{t_k} = 3,040 \text{ microinch/inch}$$

This corresponds to the design gage stress of:

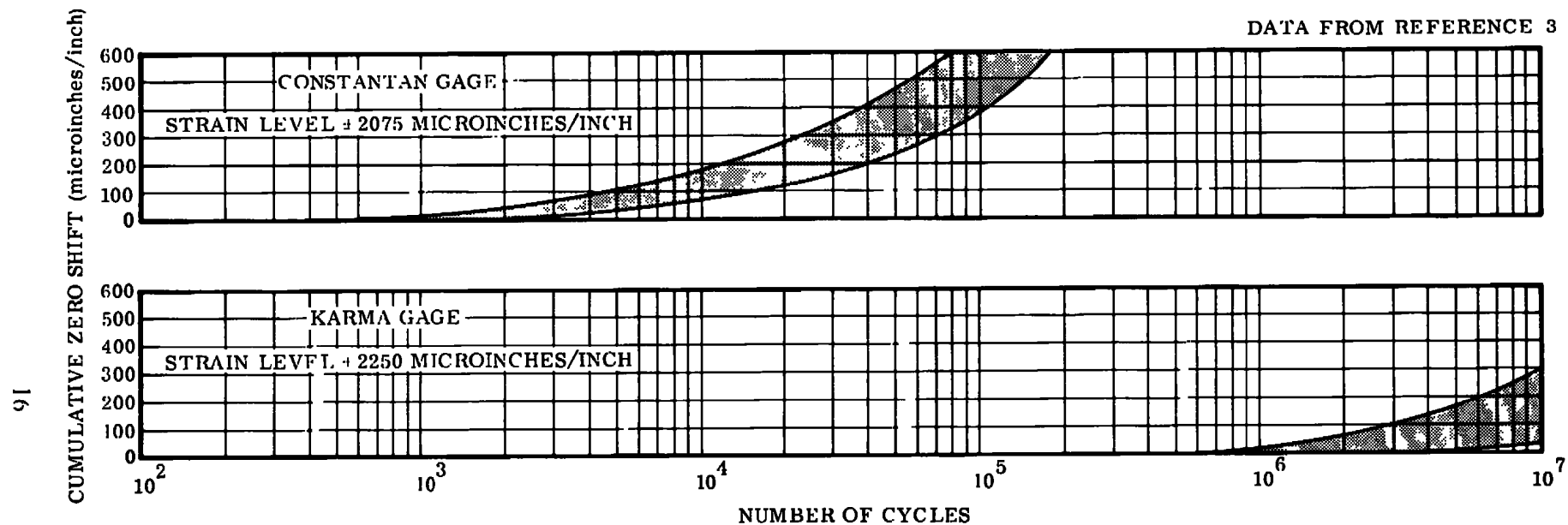
$$f_{t_k} = \frac{3,040}{1,000,000} (27,000,000) = 82,000 \text{ psi}$$

Zero compensation and modulus compensation of balance bridges will remain a requirement in the HIRT facility. Runs will be of short duration and temperature changes on the balances during runs will not be significant, but runs will occur at varying tunnel charge temperatures. With compensation for modulus and zero changes over temperature variations between -30°F and 70°F (the operating range of the tunnel), the balance calibration can be performed at room temperature and still be valid over the tunnel operating range.

Karma gages can be compensated for modulus and zero shifts. Figure 5 supports this contention by showing gage characteristics as temperature varies. Important to zero compensation is the change in apparent microstrain over the temperature range desired. As shown in Figure 5, the shifts in microstrain of the Karma gages are not significantly larger than those of the Constantan gages over the HIRT facility temperature range.

The important contribution to modulus compensation is gage factor. Gage factor is a nondimensional value proportional to the gage sensitivity. Of primary interest is that the variation of gage factor with temperature have a constant slope (Figure 5). This is true for both gages; thus the Karma gage can also be modulus compensated.

-
2. Standard Gage Selection Chart, Micro-Measurements, Vishay Intertechnology, Inc., Gage Catalog.



3. Technical Note TN-130-2, Micro-Measurements, Vishay Intertechnology, Inc., Data Sheets FR-22, April 15, 1968 and FR-35, April 15, 1968

Figure 4. Strain Gage Fatigue Life Curves

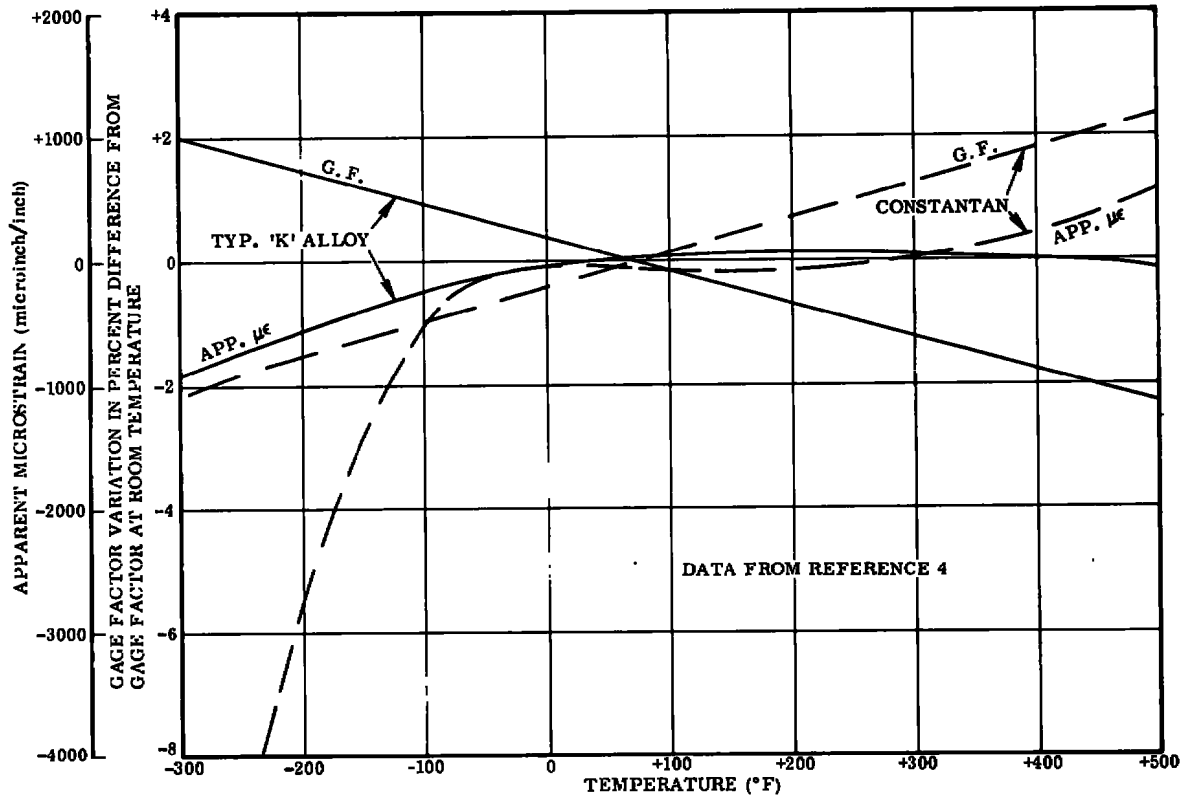


Figure 5. Apparent Strain and Gage Factor of Strain Gage Alloys versus Temperature

The disadvantage of using Karma gages is that installation costs are greater than those for Constantan gages.

4.3 SAFETY FACTORS

In many of today's wind tunnels it is standard practice to design the balance flexures for a factor of 2.00 on the yield stress. For the HIRT facility it is suggested that this criteria also be used and possibly extended to the entire two-shell balance.

The two-shell balance has three areas of potential critical stress. They are the webs, ears, and the inner rod (Figure 2).

From Figure 2 it can be seen that, should failure of the webs or ears occur, the remainder of the balance will remain intact; therefore failure will be noncatastrophic to the model and tunnel. However, failure of the inner rod would result in loss of the model. This is highly unlikely, because analysis of the inner rod (a tube) is conservative in that it does not include a form factor. It should also be noted that loss of a model will not cause catastrophic damage to the tunnel; the Ludwig tube design has no turbine/fan within the tunnel circuit.

For the above reasons, a safety factor of 2.00 on yield for all combined loads is considered to be a reasonable design criteria.

4. Technical Note TN-128, Micro-Measurements, Vishay Intertechnology, Inc., August 1968.

SECTION V

BALANCE LOAD CAPACITIES

The balance load capacities for the 1-1/2, 2-1/2, 3-1/2, and 4-1/2-inch diameter balances are given in Table 2. These load ratios are similar to those of balances in use today and proved to be typical of the requirements of HIRT facility balances. It is noted that the safety factor of the balances is based on all combined loads applied simultaneously. However, the maximum normal force and maximum pitching moment (as well as the maximum side force and maximum yawing moment) can only be applied separately unless applied as in Figure 6, a typical balance load rhombus. Several examples of allowable normal force/pitching moment combinations are shown below.

| <u>Case No.</u> | <u>Normal Force</u> | <u>Pitching Moment</u> |
|-----------------|---------------------|------------------------|
| 1 | 1.0 | 0.0 |
| 2 | 0.0 | 3.0 |
| 3 | 0.5 | 1.5 |
| 4 | 0.2 | 2.4 |

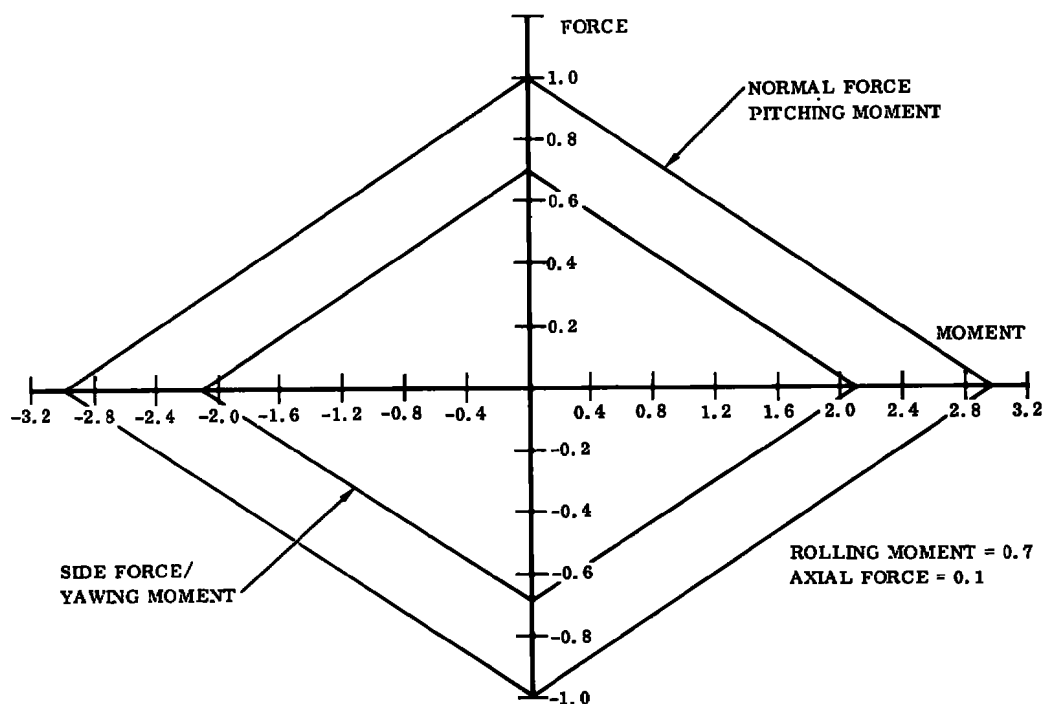
By examining the load rhombus (Figure 6) it is seen that the maximum normal force allowed on the balance occurs when the pitching moment is zero. Therefore, the placement of the balance moment center (BMC) is very important. By correctly positioning the balance, maximum use of the balance load capacities is attained. Another point for consideration is that, in repositioning the BMC for various runs of the test, more data points will generally be possible. This concept of varying BMC location can be used to attain higher normal force for given runs, thus allowing for more test points.

Figure 7 is a graphic representation of the balance capacity (in terms of normal force) as a function of balance diameter. The combined load capability (i.e., the capability with all loads applied simultaneously) curve shown is based on a safety factor of 2.00 on yield with the material at room temperature for all combined loads.

As balances are unlikely to experience full load applied in all components simultaneously, the "specified load capability" curve was added to Figure 7. It gives an example of increased capacity in selected components while eliminating others. This is a practical example where model yaw and roll are not in the test plan. In such cases normal force, pitching moment, and axial force capabilities can be increased significantly. The results of this analysis are clearly illustrated in Figure 7, Normal Force Capacity versus Balance Diameter, Figure 8, Load Rhombus, and Table 3, Balance Load Capacities.

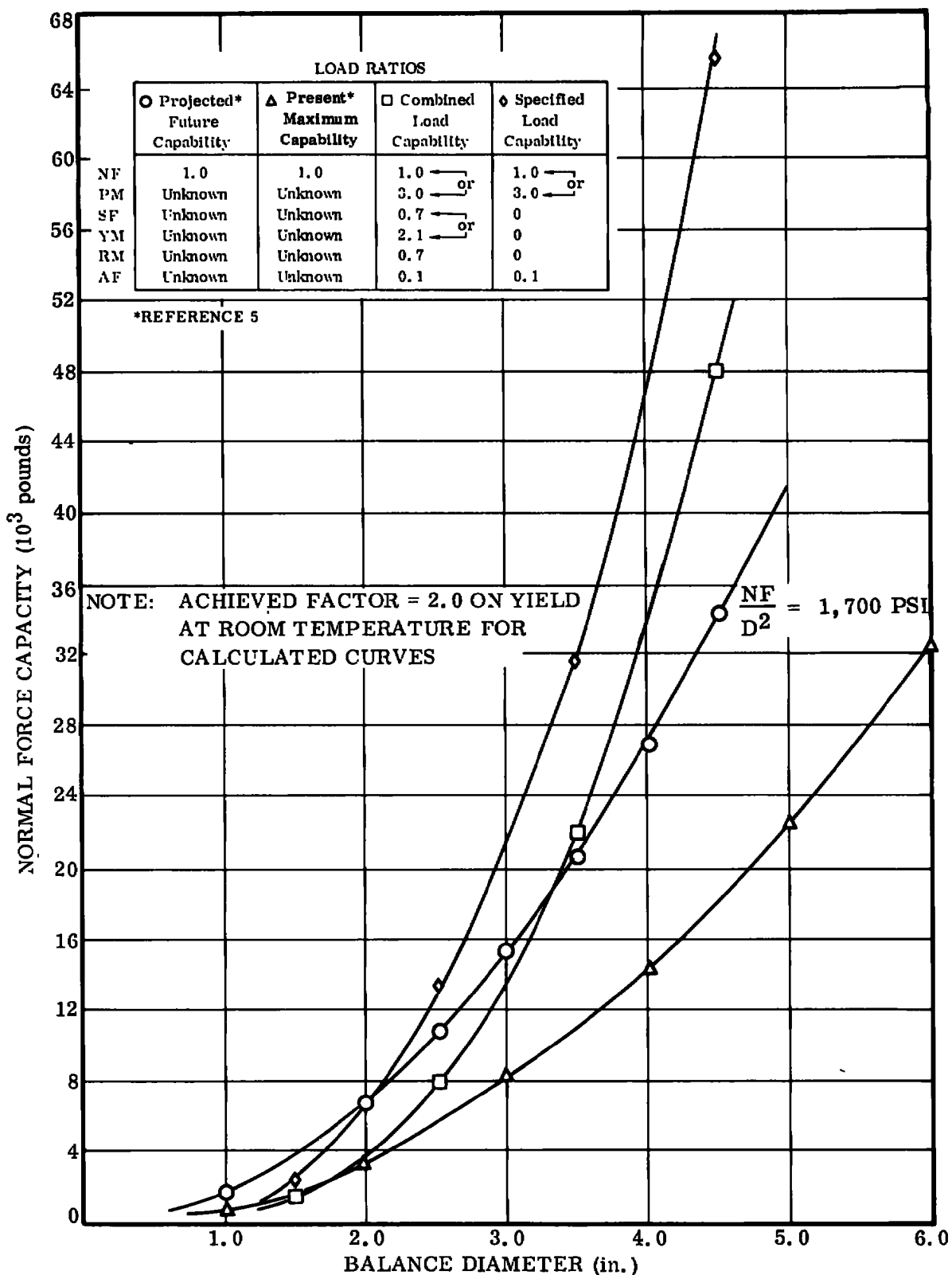
Table 2. Balance Load Ratios and Balance Loads for Combined Loading Condition (Normal Force as a Base)

| Component | Load ratios | 1.50-in.-dia balance | 2.50-in.-dia balance | 3.50-in.-dia balance | 4.50-in.-dia balance |
|----------------------------|-------------|-------------------------|-------------------------|-------------------------|-------------------------|
| Normal force (lb) | 1.00 or | 1,330 or | 7,570 or | 22,040 or | 47,900 or |
| Pitching moment (in-lb) | 3.00 or | 3,990 or | 22,710 or | 66,120 or | 143,700 or |
| Side force (lb) | 0.70 or | 931 or | 5,299 or | 15,428 or | 33,530 or |
| Yawing moment (in-lb) | 2.10 or | 2,793 or | 15,897 or | 46,284 or | 100,590 or |
| Rolling moment (in-lb) | 0.70 | 931 | 5,299 | 15,428 | 33,530 |
| Axial force (lb) | 0.10 | 133 | 757 | 2,204 | 4,790 |



NOTE: NORMAL FORCE/PITCHING MOMENT, SIDE FORCE/YAWING MOMENT, ROLLING MOMENT, AND AXIAL FORCE CAN BE APPLIED SIMULTANEOUSLY.

Figure 6. Typical Load Rhombus for Combined Loading Condition



5. "Hypersonic Research Facilities Study," McDonnell Aircraft Company, NASA CR114323, Volume II, Part I, pp. 6-52, October 2, 1970.

Figure 7. Normal Force Capacity versus Balance Diameter

Substantial increases in NF/PM are realized as shown in Table 3, varying from an increase of 37 percent for the 4.50-inch-diameter balance to 87 percent for the 1.50-inch-diameter balance. Each balance is stressed for the specified loading conditions in Section VI. These stress analyses show that the webs are critical for the 1.50- and 2.50-inch-diameter balances, the ears are critical for the 3.50-inch-diameter balance, and the inner rod and ears are critical for the 4.50-inch-diameter balance with these specified loads. Thus care must be taken in determining specialized loads to be sure that no part of the balance is overloaded.

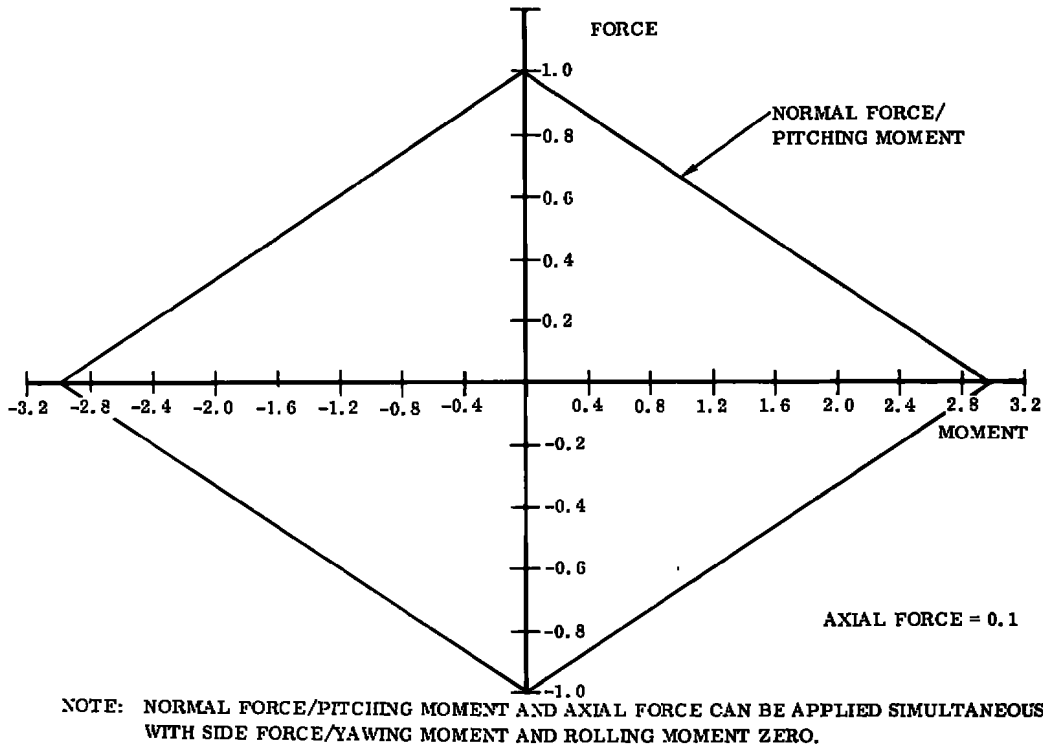


Figure 8. Typical Load Rhombus for Specified Loading Condition

For comparison, reference information from other studies is included in Figure 7. The two shell balances prove to be better than the projected future capabilities (defined as 1,700 NF/D² and the definition of high capacity) of previous studies when the balance diameter is greater than 3.00 inches, but drop below the present maximum capability curve when the balance diameter is less than 2.00 inches. Since it is likely that the HIRT facility balances will be larger than 2.00 inches in diameter, the two-shell balance appears to be a strong candidate as the primary HIRT facility balance.

The two-shell balance design has an inherent design advantage. A hole through the balance center can be provided for such items as instrumentation leads, air supply lines, or instrumentation packages. This advantage can be achieved without large load capacity losses as long as the center hole does not exceed 50 percent of the balance diameter. Figure 9 shows the effect of balance inside diameter on balance load capacity. The two-shell balance has proved to be a versatile design.

Table 3. Load Ratios and Balance Loads for Specified Loading Condition (Normal Force as a Base)

| Component | Load Ratio | 1.50-in.-dia balance | 2.50-in.-dia balance | 3.50-in.-dia balance | 4.50-in.-dia balance |
|-----------------|------------|-------------------------|-------------------------|-------------------------|-------------------------|
| Normal force | 1.0 | 2,480 | 13,475 | 31,738 | 65,620 |
| Pitching moment | 3.0 | 7,440 | 40,425 | 95,214 | 196,860 |
| Side force | 0 | 0 | 0 | 0 | 0 |
| Yawing moment | 0 | 0 | 0 | 0 | 0 |
| Rolling moment | 0 | 0 | 0 | 0 | 0 |
| Axial force | .10 | 248 | 1,347 | 3,173 | 6,562 |

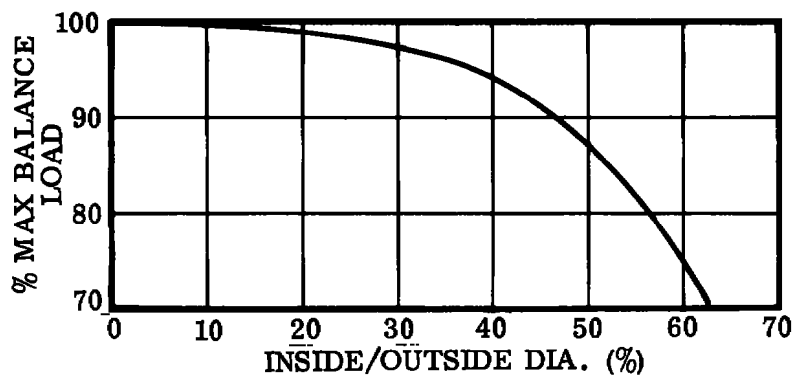


Figure 9. Effect of Center Hole on Balance Capacity

SECTION VI

STRESS ANALYSIS

The analyses performed on each of the designed balances include:

- a. Balance stress levels.
- b. Bridge outputs.
- c. Balance deflections.
- d. Working stress levels of strain gages.

A 18-Ni 300 grade maraging steel is used as a baseline material. A table of its properties is presented in Section IV, Table 1. The analyses are based on room temperature (300°K). The summary of balance data is presented in Figure 7, Section V, as a curve of normal force capacity versus balance diameter.

6.1 BALANCE STRESSES

The loads for each of the balances are presented in Table 2, Section V. A summary of safety factors on the balance is presented in Table 4.

6.1.1 Web Stress Calculations

By using compatibility equations of translational and rotational equilibrium along with the static equations of equilibrium of force and moment, the web stresses can be determined. Table 5 presents a summary of web stresses for each of the balances. The values are determined from the following systems of equations.

- a. Summation of forces equals zero (3 axes).
- b. Summation of moments equals zero (3 axes).
- c. Compatibility of translation of all parts (3 axes).
- d. Compatibility of rotation of all parts (3 axes).

These equations nearly match the experimental data collected over the past ten years. Adjustments have been made to the analytical equations to more closely match the experimental data. Research is continuing in this area to perfect the analysis. The equations are programmed at General Dynamics Convair Aerospace Division, San Diego operation, on the High Speed Wind Tunnel 1830 computer.

Table 4. Safety Factor Summary

| Item | Page | Safety Factors on Yield Stress | | | | | | | |
|----------------------|------|--------------------------------|---------------|---------------|---------------|------------------------------|---------------|---------------|---------------|
| | | Combined loading conditions | | | | Specified loading conditions | | | |
| | | 1.50 in. dia. | 2.50 in. dia. | 3.50 in. dia. | 4.50 in. dia. | 1.50 in. dia. | 2.50 in. dia. | 3.50 in. dia. | 4.50 in. dia. |
| Webs | 17 | 2.0 | 2.0 | 2.0 | 2.0 | 2.0 | 2.0 | 2.5 | 2.6 |
| Ears | 18 | 2.3 | 2.4 | 2.0 | 2.0 | 2.2 | 2.1 | 2.0 | 2.0 |
| Inner rod | 18 | 5.8 | 3.9 | 2.8 | 2.2 | 3.8 | 2.7 | 2.4 | 2.0 |
| Braze | 19 | 59.9 | 20.2 | 10.9 | 7.2 | 39.2 | 13.8 | 9.2 | 6.4 |
| Balance-to-model pin | 20 | 13.4 | 6.1 | 5.6 | 4.3 | 67.3 | 19.4 | 16.1 | 10.2 |

Note: All safety factors are based on 280,000 psi tensile yield stress and 170,000 psi shear stress.

Table 5. Summary of Web Stresses

| Item | Units | Web stresses | | | | | | | |
|--|-------|-----------------------------|---------------|---------------|---------------|------------------------------|---------------|---------------|---------------|
| | | Combined loading conditions | | | | Specified loading conditions | | | |
| | | 1.50 in. dia. | 2.50 in. dia. | 3.50 in. dia. | 4.50 in. dia. | 1.50 in. dia. | 2.50 in. dia. | 3.50 in. dia. | 4.50 in. dia. |
| Normal force aft | lb | 665 | 3,785 | 11,020 | 23,950 | 1,240 | 6,737 | 15,869 | 32,810 |
| Side force aft | lb | 465 | 2,650 | 7,714 | 16,765 | 0 | 0 | 0 | 0 |
| Rolling moment aft | lb | 818 | 4,826 | 14,013 | 30,745 | 0 | 0 | 0 | 0 |
| Axial force | lb | 133 | 757 | 2,204 | 4,790 | 248 | 1,347 | 3,173 | 6,562 |
| Normal force stress | psi | 14,695 | 15,459 | 17,201 | 18,028 | 27,775 | 27,518 | 24,770 | 24,697 |
| Side force stress | psi | 10,427 | 10,821 | 12,041 | 12,620 | 0 | 0 | 0 | 0 |
| Rolling moment stress | psi | 14,440 | 10,233 | 8,446 | 7,382 | 0 | 0 | 0 | 0 |
| Axial force stress | psi | 16,163 | 16,196 | 19,045 | 24,020 | 30,139 | 28,822 | 27,418 | 32,905 |
| Stress on side force web due to normal force | psi | 5,720 | 10,215 | 11,328 | 14,891 | 0 | 0 | 0 | 0 |
| Indeterminant structure | | | | | | | | | |
| a. S-Shape | psi | 47,310 | 49,323 | 36,431 | 30,459 | 88,217 | 87,797 | 52,461 | 41,726 |
| b. Bending | psi | 11,497 | 13,130 | 11,535 | 9,277 | 21,439 | 23,372 | 16,611 | 12,709 |
| Total web stress | psi | 139,975 | 139,946 | 139,999 | 140,010 | 139,713 | 139,991 | 111,465 | 109,316 |

6.1.2 Ear Stresses

The analysis of the two-shell balance ears is best illustrated by referring to Figure 2. It is shown that all loads in the webs must pass through the ears. The ear root is the critical section of the ear. Table 6 is a summary of the ear stresses of the de-signed balances.

6.1.3 Inner Rod Stresses

The critical section of the inner rod is Section D-D of Figure 2. Table 7 is a summary of the inner rod stresses.

Table 6. Ear Stresses

| Item | Units | Dimensions and stresses | | | | | | | |
|-------------------------|-------|-----------------------------|---------------|---------------|---------------|------------------------------|---------------|---------------|---------------|
| | | Combined loading conditions | | | | Specified loading conditions | | | |
| | | 1.50 in. dia. | 2.50 in. dia. | 3.50 in. dia. | 4.50 in. dia. | 1.50 in. dia. | 2.50 in. dia. | 3.50 in. dia. | 4.50 in. dia. |
| Outside radius (R) | in. | 0.735 | 1.235 | 1.735 | 2.235 | 0.735 | 1.235 | 1.735 | 2.235 |
| Inside radius (RI) | in. | 0.590 | 0.940 | 1.225 | 1.515 | 0.590 | 0.940 | 1.225 | 1.515 |
| Ear length (EARLG) | in. | 0.232 | 0.366 | 0.547 | 0.710 | 0.232 | 0.366 | 0.547 | 0.710 |
| Bending stresses | | | | | | | | | |
| a. STOT1 (pt. A) | psi | 100,225 | 103,331 | 126,560 | 129,084 | 113,744 | 116,246 | 122,471 | 120,839 |
| b. STOT2 (pt. B) | psi | 37,145 | 38,763 | 60,450 | 61,489 | 113,744 | 116,246 | 122,471 | 120,839 |
| Torsional stress | psi | 40,757 | 35,152 | 34,080 | 30,447 | 34,109 | 41,585 | 41,092 | 41,329 |
| Safety factor | — | 2.3 | 2.4 | 2.0 | 2.0 | 2.2 | 2.1 | 2.0 | 2.0 |

Table 7. Inner Rod Stresses

| Item | Units | Stress | | | | | | | |
|---|-------|-----------------------------|---------------|---------------|---------------|------------------------------|---------------|---------------|---------------|
| | | Combined loading conditions | | | | Specified loading conditions | | | |
| | | 1.50 in. dia. | 2.50 in. dia. | 3.50 in. dia. | 4.50 in. dia. | 1.50 in. dia. | 2.50 in. dia. | 3.50 in. dia. | 4.50 in. dia. |
| Inner rod bending | psi | 48,269 | 71,060 | 100,757 | 124,150 | 73,785 | 103,719 | 118,991 | 139,504 |
| Inner rod shear (due to rolling moment) | psi | 3,159 | 4,271 | 5,548 | 6,327 | 0 | 0 | 0 | 0 |
| Safety factor | — | 5.8 | 3.9 | 2.9 | 2.2 | 3.8 | 2.7 | 2.4 | 2.0 |

Table 8. Brazed Joint Analysis

| Item | Units | Dimensions and stresses | | | | | | | |
|-------------------------|-------|-----------------------------|---------------|---------------|---------------|------------------------------|---------------|---------------|---------------|
| | | Combined loading conditions | | | | Specified loading conditions | | | |
| | | 1.50 in. dia. | 2.50 in. dia. | 3.50 in. dia. | 4.50 in. dia. | 1.50 in. dia. | 2.50 in. dia. | 3.50 in. dia. | 4.50 in. dia. |
| Inside diameter socket | in. | 1.18 | 1.88 | 2.45 | 3.03 | 1.18 | 1.88 | 2.45 | 3.03 |
| Outside diameter socket | in. | 1.47 | 2.47 | 3.47 | 4.47 | 1.47 | 2.47 | 3.47 | 4.47 |
| Socket length | in. | 1.13 | 1.38 | 1.63 | 1.88 | 1.13 | 1.38 | 3.47 | 1.88 |
| Shear in socket | psi | 811.7 | 4,620 | 13,452 | 29,235 | 1,240 | 6,738 | 15,869 | 32,810 |
| Moment in socket | in-lb | 188.7 | 1,691 | 7,356 | 20,771 | 288 | 2,466 | 8,680 | 23,312 |
| Total shear stress | psi | 5,497 | 14,619 | 24,257 | 35,128 | 8,396 | 21,318 | 28,616 | 39,423 |
| Safety factor | — | 30.9 | 11.6 | 7.0 | 4.8 | 20.2 | 8.0 | 5.9 | 4.3 |

6.1.4 Brazed Joint Stresses

The balance brazed joints are assumed to be simple socket joints with no braze. Using this conservative assumption, the joint is analyzed using a method given in the General Dynamics Convair Aerospace division Experimental Aerodynamics Design Manual, dated April 14, 1958. A summary of the analysis is presented in Table 8. This table shows that the brazed joint is not critical.

6.1.5 Balance-to-Model Pins

Assuming that the balance-to-model pins are made of materials with 170,000 psi ultimate shear stress, and that two model pins are used (top and bottom), a summary of the analysis is presented in Table 9.

Table 9. Balance-to-Model Pin Analysis

| Item | Units | Dimensions and stresses | | | | | | | |
|-------------------------|------------------|-----------------------------|---------------|---------------|---------------|------------------------------|---------------|---------------|---------------|
| | | Combined loading conditions | | | | Specified loading conditions | | | |
| | | 1.50 in. dia. | 2.50 in. dia. | 3.50 in. dia. | 4.50 in. dia. | 1.50 in. dia. | 2.50 in. dia. | 3.50 in. dia. | 4.50 in. dia. |
| Pin diameter | in. | 0.250 | 0.313 | 0.438 | 0.500 | 0.250 | 0.313 | 0.438 | 0.500 |
| Total shear load | lb | 624 | 2,153 | 4,543 | 7,826 | 124 | 673 | 1,586 | 3,281 |
| Total pin cross section | in. ² | 0.049 | 0.077 | 0.151 | 0.196 | 0.049 | 0.077 | 0.151 | 0.196 |
| Total pin stress | psi | 12,716 | 27,983 | 30,156 | 39,860 | 2,526 | 8,753 | 10,529 | 16,710 |
| Safety factor | — | 13.4 | 6.1 | 5.6 | 4.3 | 67.3 | 19.4 | 16.1 | 10.2 |

6.2 BRIDGE OUTPUTS

The bridge outputs of each component of the balance are given in Table 10. These outputs are determined assuming the gage factor of the strain gages to be 2.08.

Table 10. Bridge Outputs

| Item | Bridge outputs (millivolts/volt) | | | | | | | |
|----------------------|----------------------------------|---------------|---------------|---------------|------------------------------|---------------|---------------|---------------|
| | Combined loading conditions | | | | Specified loading conditions | | | |
| | 1.50 in. dia. | 2.50 in. dia. | 3.50 in. dia. | 4.50 in. dia. | 1.50 in. dia. | 2.50 in. dia. | 3.50 in. dia. | 4.50 in. dia. |
| Normal force forward | 1.147 | 1.190 | 1.325 | 1.388 | 2.139 | 2.119 | 1.908 | 1.902 |
| Normal force aft | 1.147 | 1.190 | 1.325 | 1.388 | 2.139 | 2.119 | 1.908 | 1.902 |
| Side force forward | 0.803 | 0.833 | 0.927 | 0.972 | 0 | 0 | 0 | 0 |
| Side force aft | 0.803 | 0.833 | 0.927 | 0.972 | 0 | 0 | 0 | 0 |
| Rolling moment | 0.650 | 0.432 | 0.358 | 0.310 | 0 | 0 | 0 | 0 |
| Axial force | 0.885 | 0.856 | 0.866 | 0.856 | 1.614 | 1.527 | 1.247 | 1.172 |

6.3 BALANCE DEFLECTION

Estimated balance deflections are calculated as angular deflections of the two-shell balances. Table 11 is a summary of these estimates both in terms of full capacity force and moment and in terms of unit force and moment.

6.4 BALANCE GAGE STRESS

The maximum gage stress for each of the balances is presented in Table 12. This stress will occur only under simultaneous application of all loads for the selected load condition. The single-gage process used at General Dynamics is a form of proof-loading to verify web and gage stress. The 1.50- and 2.50-inch-diameter balances require special care when selecting gages for the bridges, since some potentially

usable gages will have stresses larger than desirable. For these balances, gages with lower stresses will be chosen to complete the bridges. Sometimes this will increase interactions, but the accuracy can be retained through calibration. The desirable gage stress for Karma gages is below 82,000 psi since the fatigue life falls below 4×10^4 cycles above it.

Table 11. Balance Deflections

| Item | Angular deflections (minutes) | | | | | | | |
|----------------------------------|-------------------------------|---------------|---------------|---------------|------------------------------|---------------|---------------|---------------|
| | Combined loading conditions | | | | Specified loading conditions | | | |
| | 1.50 in. dia. | 2.50 in. dia. | 3.50 in. dia. | 4.50 in. dia. | 1.50 in. dia. | 2.50 in. dia. | 3.50 in. dia. | 4.50 in. dia. |
| Angle/pound normal force | 0.018201 | 0.003025 | 0.001157 | 0.000560 | 0.018201 | 0.003025 | 0.001157 | 0.000550 |
| Angle/inch-pound pitching moment | 0.005480 | 0.000880 | 0.000330 | 0.000152 | 0.005480 | 0.000880 | 0.000330 | 0.000152 |
| Angle/full scale normal force | 24.2 | 22.9 | 25.5 | 26.8 | 45.1 | 40.8 | 36.7 | 36.1 |
| Angle/full scale pitching moment | 21.9 | 20.0 | 21.8 | 21.8 | 40.9 | 35.6 | 31.4 | 29.9 |

Table 12. Balance Gage Stress

| Item | Stresses (psi) | | | | | | | |
|-----------------------|-----------------------------|---------------|---------------|---------------|------------------------------|---------------|---------------|---------------|
| | Combined loading conditions | | | | Specified loading conditions | | | |
| | 1.50 in. dia. | 2.50 in. dia. | 3.50 in. dia. | 4.50 in. dia. | 1.50 in. dia. | 2.50 in. dia. | 3.50 in. dia. | 4.50 in. dia. |
| Maximum gage stresses | 82,000 | 82,000 | 74,379 | 64,555 | 82,295 | 80,234 | 47,161 | 34,530 |

SECTION VII

BALANCE-TO-STING JOINT

Two balance-to-sting joint concepts were analyzed. The clutch face joint is shown to be larger in overall diameter for a given load condition than the taper joint; however, the taper joint is longer. The balance-to-sting attachment is designed using both concepts for a direct comparison.

7.1 CLUTCH FACE JOINT

The analysis of the clutch face joint shown in Figure 10 for the 3.50-inch-diameter balance designed in this study is given below. The selected specified loading condition is considered to be the most critical.

Check of bending at Section A-A:

$$M_1 = 31,738 (8.900) = 282,468 \text{ in-lb}$$

$$I = (\pi/64) (2.750^4 - 0.390^4) = 2.805 \text{ in.}^4$$

$$C = 1.375 \text{ in.}$$

$$f_b = \frac{M_1 C}{I} = 138,474 \text{ psi}$$

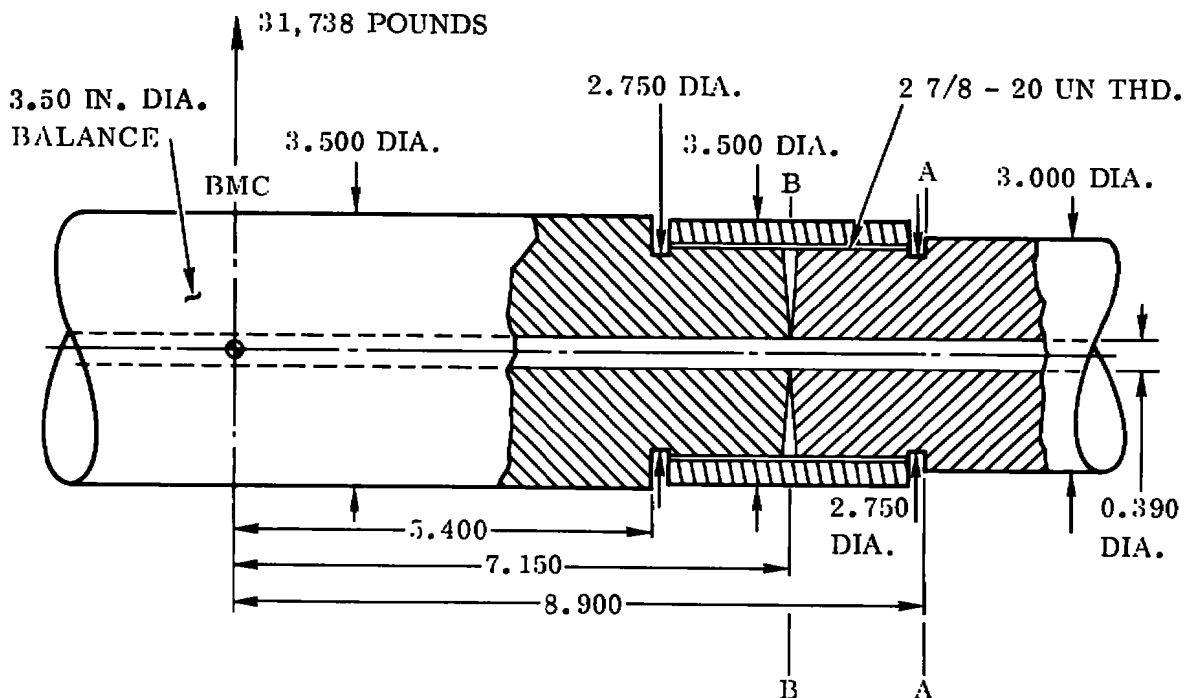


Figure 10. Clutch Face Joint for 3.50-in.-dia. Balance

Stress at Section A-A due to axial force:

$$f_t = P/A = \frac{1,347}{\frac{\pi}{4} (2.75^2 - 0.39)^2} = 232 \text{ psi}$$

Safety factor of Section A-A:

$$\text{S.F.} = \frac{F_{ty}}{f_{t\text{total}}} = \frac{280,000}{(138,474 + 232)} = \underline{\underline{2.019}}$$

Bending stress of collar with the outside diameter of 3.500 and the maximum internal diameter of 2.875:

$$M_2 = 31,738 (7.150) = 226,927 \text{ in-lb}$$

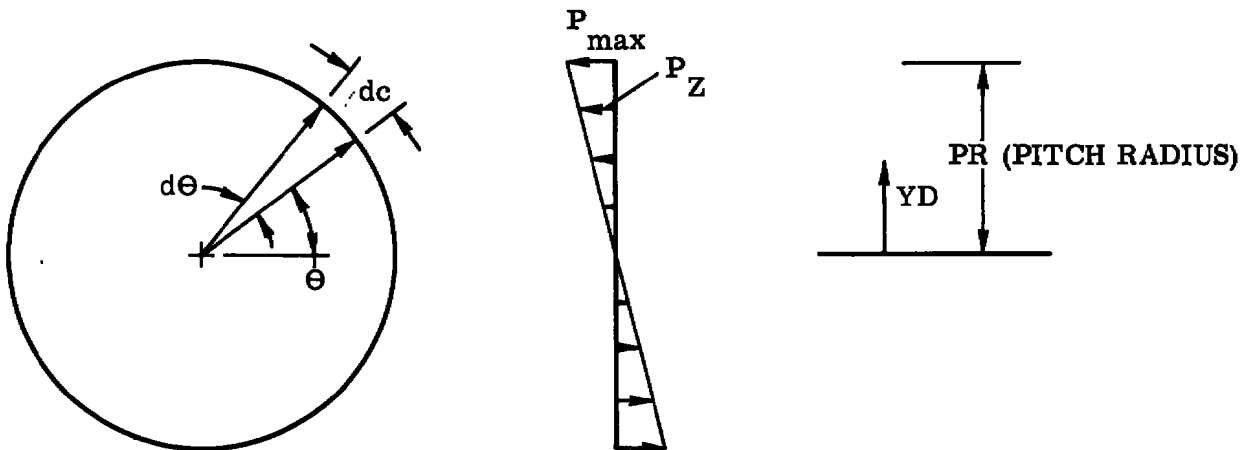
$$C = 1.750 \text{ in.}$$

$$I = (\pi/64) (3.500^4 - 2.875^4) = 4.010 \text{ in.}^4$$

$$f_b = \frac{M_2 C}{I} = \frac{226,927(1.750)}{4.010} = 99,022 \text{ psi}$$

$$\text{S.F.} = \frac{280,000}{99,022} = \underline{\underline{2.828}}$$

Assume that the collar does not precompress the clutch faces. The moment then must be reacted by the threads.



$$P_Z = \frac{YD}{PR} P_{\max} = \frac{\text{lb force}}{\text{in. circumference}}$$

$$YD = PR \sin \theta$$

$$dc = PR d\theta$$

$$\begin{aligned} M_{\text{thread}} &= 4 \int_0^{\pi/2} (P_Z dc) YD \\ &= 4 \int_0^{\pi/2} \left(\frac{YD}{PR} P_{\max} \right) (PR) d\theta (YD) \\ &= 4 \int_0^{\pi/2} (YD)^2 P_{\max} d\theta \\ &= 4 \int_0^{\pi/2} (PR)^2 P_{\max} \sin^2 \theta d\theta \\ &= 4 (PR)^2 P_{\max} \left[\frac{1}{2} \theta - \frac{1}{4} \sin 2\theta \right]_0^{\pi/2} \\ &= 4 (PR)^2 P_{\max} \left[\frac{\pi}{4} + \frac{1}{4} - \frac{1}{4} \right] \\ &= \pi (PR)^2 P_{\max} \end{aligned}$$

$$M_{\text{thread}} = M_2$$

$$P_{\max} = M_2 / \pi (PR)^2$$

$$f_{s_{\text{thread}}} = \frac{P_{\max}}{A_s / 2\pi(PR)}$$

where A_s is the thread shear area

$$A_s = \pi n L_e K_{n_{\max}} \left[\frac{1}{2n} + 0.57735 (E_{s_{\min}} - K_{n_{\max}}) \right]$$

$$n = \text{threads per inch} = 20$$

$$L_e = 1.50 \text{ in.}$$

$$K_n = 2.8209$$

$$E_s = 2.8425$$

$$A_s = \pi (20) (1.50) (2.8209) [0.1 + 0.57735 (2.8425 - 2.8209)] = 29.887$$

$$f_{s_{\text{thread}}} = \frac{2M_2 \pi R}{\pi R^2 A_s} = \frac{2M_2}{R A_s} = \frac{2 (282,468)}{1.4212 (29.887)}$$

$$= \underline{\underline{13,300 \text{ psi}}}$$

7.2 TAPER JOINT

The analysis of the taper joint shown in Figure 11 for the 3.50-inch-diameter balance is given below. As for the clutch face joint, the selected specified loading condition is considered the most critical.

Check of bending at Section D-D:

$$P = 31,738 \text{ lb}$$

$$M = 31,738 (5.400) = 171,385 \text{ in-lb}$$

$$C = 1.225 \text{ in.}$$

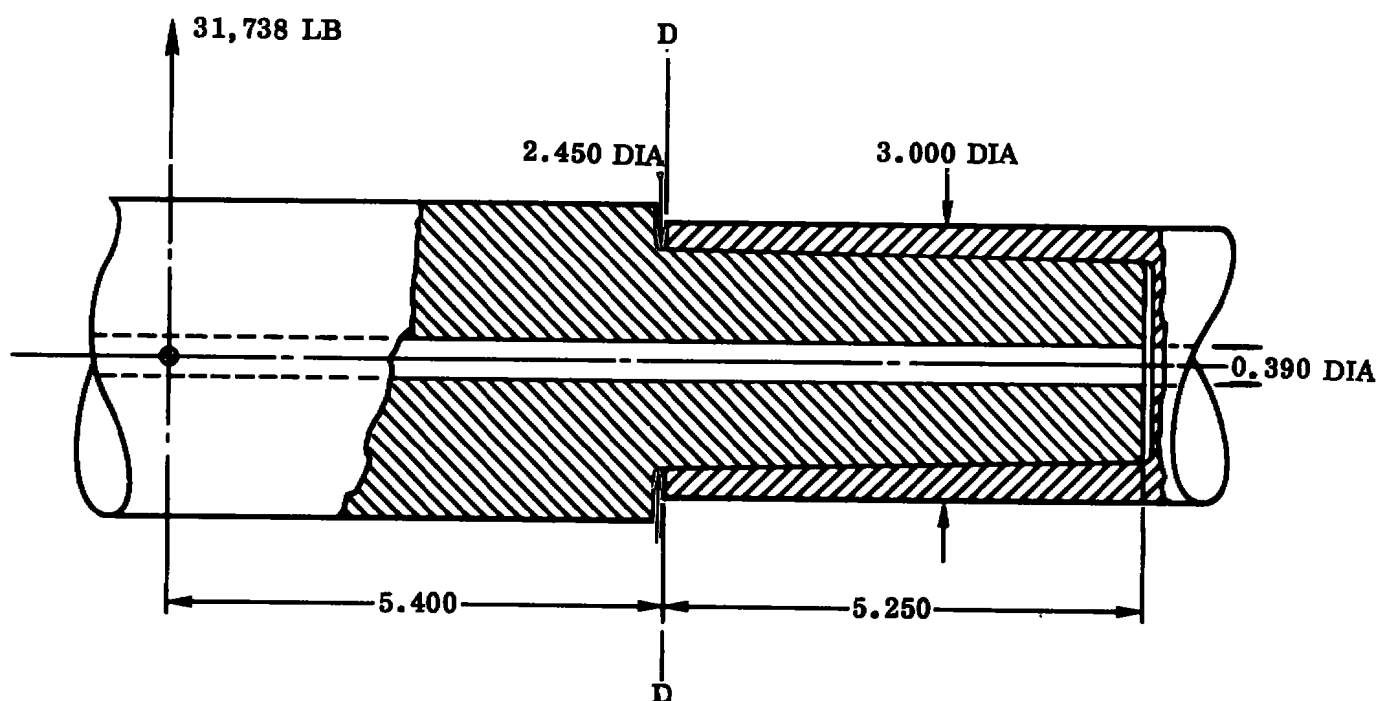


Figure 11. Taper Joint for 3.50-in.-dia. Balance

$$I = \frac{\pi}{64} (2.450^4 - 0.390^4) = 1.767 \text{ in.}^4$$

$$f_b = \frac{MC}{I} = \frac{171,385 (1.225)}{1.767} = 118,815 \text{ psi}$$

$$\text{S.F.} = \frac{280,000}{118,815} = \underline{\underline{2.357}}$$

Check of shear-out of socket:

$$R = 1.500$$

$$D = 2.450$$

$$TL = \text{Taper Length} = 5.250$$

$$M = \left[\frac{1}{2} w_M \left(\frac{TL}{2} \right) \right] \frac{2}{3} (TL) = \frac{w_M (TL)^2}{6}$$

$$w_M = \frac{6M}{(TL)^2}$$

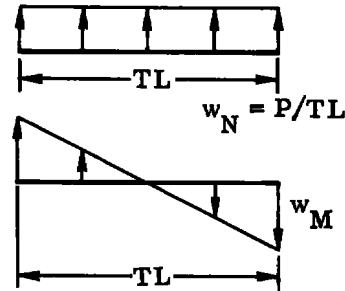
$$w_N = \frac{P}{TL} = \frac{31,738}{5.25} = 6,045 \text{ lb/in.}$$

$$w_M = \frac{6M}{(TL)^2} = \frac{6(171,385)}{(5.25)^2} = 37,308 \text{ lb/in.}$$

$$X = (2R-D)/2 = 0.345$$

$$f_s = \frac{w_N + w_M}{2X} = \frac{6,045 + 37,308}{0.690} = 62,836$$

$$\text{S.F.} = \frac{170,000}{62,836} = \underline{\underline{2.71}}$$



7.3 COMPARISON OF BALANCE-TO-STING JOINTS

The clutch face joint designed for the 3.50-inch-diameter balance is shown to be 3.500 inches in diameter for a safety factor of 2.828 on the collar, assuming that the clutch faces are not precompressed. This is unrealistic since a tight joint is needed. Therefore, to precompress the clutch faces, the collar will have a tensile stress equal to the prestress of the clutch faces. This will decrease the collar safety factor.

The taper joint of the 3.50-inch-diameter balance has been shown to be 3.000 inches in diameter for a safety factor of 2.157 on the sting.

The taper joint appears to have a clear advantage over the clutch face joint since a truly tight joint is achieved with a 0.50 inch smaller 3.00-inch-diameter joint.

SECTION VIII

COMPARISON OF BALANCE COST ESTIMATES

The estimated cost of developing balances for the HIRT facility will be greater than that for present transonic wind tunnel balances by approximately 20 percent. The principal reasons for the increased costs are:

- a. Increase in number of fabrication steps.
- b. Increase of calibration effort due to higher loads.
- c. Increased task in gaging due to Karma gage installation.

This projected cost increase does not include the additional effort of calibration should it be determined that inertial compensation is necessary. To date, this need has not been established as a requirement. This problem will undoubtedly be a function of the dynamics of the model, balance, sting, and tunnel support system.

Excluded from this estimate is the cost of new calibration equipment and the costs relative to calibration of balances in the tunnel. This new class of balance will require calibration rigs with a capacity of 65,000 pounds. The present maximum standard is 15,000 pounds and new equipment is a necessity.

SECTION IX

ESTIMATE OF BALANCE ACCURACY

While there will likely be some degradation of accuracy for the proposed high capacity (HIRT) balances as compared with present-day low load balances, it is felt that considerable improvements can be made over the accuracies achieved with prototype high capacity balances.

Table 13 summarizes the accuracies of three existing two-shell balances. One is a comparatively low load balance (C-20-2.50-D) and the other two (C-18-1.50-C and C-120-2.50-A) are prototype high capacity balances. These balances have each gone through an eleven station calibration in the normal force and side force planes. While the multi-station calibration indicates larger standard deviation errors than a three station calibration, the final result is a more accurate set of balance constants since any induced error not caused by the balance will tend to be averaged out. Also the standard deviations derived from multi-station loadings are a good indication of balance accuracy.

Table 13. Standard Deviations (1 σ) of Three Two-Shell Balances

| Component Loads | Balance | Component Accuracy (Percent of Full Scale) | | | | | |
|-----------------|--------------|--|-----------------------|------------------|---------------------|----------------------|-------------------|
| | | Normal Force Error | Pitching Moment Error | Side Force Error | Yawing Moment Error | Rolling Moment Error | Axial Force Error |
| Axial Force | C-20-2.50-D | 0.022 | 0.066 | 0.018 | 0.041 | 0.013 | 0.072 |
| | C-18-1.50-C | 0.028 | 0.057 | 0.064 | 0.067 | 0.040 | 0.048 |
| | C-120-2.50-A | 0.02 | 0.05 | 0.02 | 0.03 | 0.05 | 0.07 |
| Rolling Moment | C-20-2.50-D | 0.031 | 0.039 | 0.066 | 0.185 | 0.065 | 0.221 |
| | C-18-1.50-C | 0.061 | 0.085 | 0.107 | 0.230 | 0.089 | 0.347 |
| | C-120-2.50-A | 0.04 | 0.08 | 0.04 | 0.10 | 0.04 | 0.51 |
| Normal Force | C-20-2.50-D | 0.103 | 0.283 | 0.059 | 0.299 | 0.223 | 0.275 |
| | C-18-1.50-C | 0.136 | 0.231 | 0.219 | 0.375 | 0.067 | 0.422 |
| | C-120-2.50-A | 0.10 | 0.28 | 0.16 | 0.36 | 0.16 | 0.59 |
| Side Force | C-20-2.50-D | 0.035 | 0.081 | 0.055 | 0.183 | 0.117 | 0.144 |
| | C-18-1.50-C | 0.069 | 0.140 | 0.120 | 0.289 | 0.075 | 0.403 |
| | C-120-2.50-A | 0.07 | 0.12 | 0.15 | 0.34 | 0.19 | 0.64 |

General Dynamics has developed practical experience in the field of high capacity balances. Two proto-type designs of interest are the C-18-1.50-C and C-120-2.50-A two-shell balances. Table 13 gives the first standard deviation data of the C-18-1.50-C and the C-120-2.50-A. Although neither balance was designed for the maximum load possible from its diameter, they approach the Combined Load Capability curve in Figure 7.

When reviewing the first standard deviation data of these proto-type high capacity balances the principal errors occur in axial force from loading rolling moment, normal force, and side force. A possible source for this error can be seen from the single gage readings of the individual axial force gages. In most cases the stress level under the axial force gages due to interactions is greater than the stress caused by the axial force loading itself. The proposed HIRT balances, however, are designed such that the axial force gages experience higher stresses for axial force loadings and less stress for the interaction loadings. This will improve the balance accuracy of axial force when loading interactions.

Other possible ways to improve the standard deviation is to review the calibration methods. In particular, the mechanical advantage overhead beam used when calibrating the C-120-2.50-A balance may have induced some axial force to the balance. In addition problems with the calibration equipment have subsequently been revealed.

Existing precision calibration rigs in the United States do not have the capacity for full calibration of the HIRT balances. The only recourse is to load the balance to maximum rig capability and extrapolate the data to full balance loads. This would induce error in the balance constants. Therefore when balances with capacities larger than 15000 pounds are fabricated careful consideration must be given to the calibration of the balances.

From all indications the expected accuracy of the HIRT balances proposed here will be 0.30 to 0.40 percent of full-scale axial force for rolling moment, normal force, and side force loadings. This estimated accuracy is not as good as the present-day transonic-tunnel balance but is better than the prototype high capacity balances.

SECTION X

CONCLUSIONS

The results of this study indicate that six-component internal strain gage balances can be developed for testing in the proposed HIRT facility using contemporary materials and fabrication techniques.

The two-shell balance concept is the chosen baseline. The chief advantages of this type of balance are high stiffness, failsafe features, and the versatility of design provided by the hole through the balance center. Although the two-shell balance has these advantages, some restrictions have arisen in using it as the baseline design. For diameters below 3.00 inches, the two-shell does not meet the defined requirement ($NF/D^2 = 1,700$ psi) of high-capacity balances.

The baseline material selected for the HIRT facility is 18-Ni 300 grade double maraging steel. Past experience has shown this material to meet balance requirements.

Karma strain gages are proposed for HIRT as the gage type because of the improved fatigue life over the Constantan gage (the standard of the industry). With these gages, the designer can make better use of the high-strength steels and therefore develop higher load capacity balances.

While there will be degradation of accuracy in the proposed balances as compared with present-day low load balances, it is felt that this degradation can be minimized with further experience with high-capacity balances. Also the degradation in accuracy when data points less than full scale are taken will remain the same as for the present-day balances.

In some cases where the test schedule is limited by the balance load capacity, it has been shown that there are two possible ways to increase the effective balance capacity. First, the balance can be moved in the model to reduce the balance pitching moment and thus increase the normal force allowable. Secondly, in tests where side force, yawing moment, and rolling moment are less than maximum, the normal force, pitching moment, and axial force allowables can be proportionally increased.

Calibration of the HIRT balances will produce new problems. Certainly, new calibration equipment (and possibly new methods) will be required, both in the calibration area and within the tunnel for check calibrations. Large balance loads will make automatic loading a necessity.

Consideration should also be given to protecting the balance from the tunnel environment. By controlling the local conditions balance accuracies can be maintained because:

- a. The material properties will allow higher balance loads.
- b. The chance of balance errors from transient temperature conditions due to air blowing across gage locations will be greatly reduced.
- c. Special procedures needed to prevent wires from disengaging due to air blowing through the balance could be eliminated.
- d. The possible pressure on the strain gages is eliminated.

The need for inertial compensation is a problem that also needs careful consideration. It appears that some model/balance/sting/tunnel support systems may not require inertial compensation. It may be that other systems need inertial compensation only when certain pitch/pause rates are exceeded.

The balance/sting joints presented in this study are tapers. A review of clutch face designs shows a disadvantage in the joint diameter size.

It is estimated that the basic balance cost will be approximately 20 percent higher excluding any additional costs for inertial compensation that may be required.

ABBREVIATIONS AND SYMBOLS

| <u>Symbol</u> | <u>Nomenclature</u> | <u>Units</u> |
|----------------|---|---------------------|
| A | Distance from BMC to front of balance | in. |
| B | Overall length from front of balance through second fastened section (Figure 2) | in. |
| BRAZ L | Fastened joint length of two parts | in. |
| BMC | Balance moment center | — |
| C | Length of key slot | in. |
| DIA | Balance bearing surface diameter (maximum diameter of balance) | in. |
| DISTW | Distance between the web sections | in. |
| E | Modulus of elasticity | ksi |
| EARLG | Length of ears on balance | in. |
| °F | Fahrenheit | deg |
| G | Modulus of rigidity | ksi |
| GF | Gage factor | |
| HIRT | High Reynolds Number Transonic Wind Tunnel | |
| Key Slot | Width of key slot | in. |
| Overall Length | Overall length of balances | in. |
| Pin Dimensions | Pin diameter and depth | in. |
| PR | Pitch radius | in. |
| R | Outside radius of outer shell | in. |
| RI | Inside radius of outer shell | in. |
| SLOT | Distance between parallel webs | in. |
| Split Cut | Cut to separate shells | in. |
| STOT1 | Ear stress at likely critical point (Pt. A) | lb/in. ² |
| STOT2 | Ear stress at second possible critical point (Pt. B) | lb/in. ² |
| TAPER | Variation on diameter of taper | in./ft |

ABBREVIATIONS AND SYMBOLS (Contd)

| <u>Symbol</u> | <u>Nomenclature</u> | <u>Units</u> |
|----------------------|--|----------------------------|
| Taper Length | Overall length of engagement of taper | in. |
| Taper Major Diameter | Maximum diameter of taper | in. |
| Taper Minor Diameter | Minimum diameter of taper | in. |
| TIRID | Inside diameter of inner rod | in. |
| TIRN | Outside diameter of inner rod | in. |
| TNOPW | Number of parallel webs | — |
| TOSID | Outer shell inside diameter | in. |
| TOSOD | Outer shell outside diameter | in. |
| WL | Web length | in. |
| WT | Web thickness | in. |
| WW | Web Width | in. |
| Y | Distance between webs | in. |
| F_{tu} | Ultimate tensile stress | ksi |
| F_{ty} | Tensile yield stress | ksi |
| F_{su} | Ultimate shear stress | ksi |
| f_{tc} | Tensile stress allowable on Constantan gages | psi |
| f_{tk} | Tensile stress allowable on Karma gages | psi |
| ϵ_{tc} | Strain level allowable on Constantan gages | $\mu\text{in.}/\text{in.}$ |
| ϵ_{tk} | Strain level allowable on Karma gages | $\mu\text{in.}/\text{in.}$ |
| $\mu\epsilon$ | Microstrain | $\mu\text{in.}/\text{in.}$ |